EGYPTIAN ACADEMIC JOURNAL OF
BIOLOGICAL SCIENCES
ENTOMOLOGY

A

ISSN
1687-8809

WWW.EAJBS.EG.NET

Vol. 12 No. 3 (2019)

Egyptian Academic Journal of Biological Sciences is the official English language journal of the Egyptian Society for Biological Sciences, Department of Entomology, Faculty of Sciences Ain Shams University.
Entomology Journal publishes original research papers and reviews from any entomological discipline or from directly allied fields in ecology, behavioral biology, physiology, biochemistry, development, genetics, systematics, morphology, evolution, control of insects, arachnids, and general entomology.
www.eajbs.eg.net

In Vitro Assessment of Antimicrobial Activity of Chitosan Nanoparticles Loaded with the Honeybee, *Apis mellifera* Venom

Mostafa I. Hassan[1], S.I.El-dek[2,*], Aly F. Mohamed[3], and Abdelwahab Khalil Abdelwahab [4]

1.Department of Zoology and Entomology, Faculty of Science, Al-Azhar University, Nasr City, Cairo, Egypt
2. Materials Science and Nanotechnology Department, Faculty of Postgraduate Studies for Advanced Sciences (PSAS), Beni-Suef University, Beni-Suef 62511, Egypt
3Applied Researches Sector, Vacsera, Giza, Egypt
4.Zoology Department, Faculty of Science, Beni-Suef University, Beni-Suef, Egypt
Email: *samaa@psas.bsu.edu.eg; didi5550000@gmail.com*

_____

ABSTRACT

The aim of the present study was to extract chitosan from corpses of the naturally died honeybee, prepare chitosan nanoparticles (B- CS-NPs) for loading the honeybee, *Apis mellifera* venom (BV) and evaluate their antimicrobial potential. Chitin was extracted from the cuticle of corpses of naturally died honeybees following 4 steps; de-waxing, demineralization, deproteinization and discoloration. Chitosan was obtained by deacetylation of chitin and characterized using the Fourier transform infrared (FTIR) and X-ray diffraction. Honeybee chitosan nanoparticles (B-CS-NPs) were prepared by ionic gelation method using TPP in acidic medium. Empty nanoparticles (B-CS-NPs) and bee venom loaded nanoparticles (BV loaded NPs) were characterized. Hydrodynamic size and zeta potential of B- CS NPs were 74.2 nm, and 51.1 mV, while those of bee venom-loaded (BV loaded NPs) were 110.5 nm, 49.0 mv, respectively. The loading capacity (LC) and encapsulation efficiency (EE) were 86.5 % and 91.3 %, respectively, at bee venom concentration of 600 μg / ml. The antimicrobial activity of empty and BV loaded nanoparticles was studied using different strains of human pathogenic bacteria and fungi. Compared to empty nanoparticles, BV loaded NPs exhibited potent antimicrobial activity against the studied strains except in *Aspergillus flavus* fungus, which seemed to be resistant.

INTRODUCTION

Most studies isolated and characterized chitin and chitosan from the shells of crustaceans since this is the most easily available substance for large-scale processing. However, recent reports stated the possibility of getting chitin and chitosan from the cuticle of insects. Although, these sources are not suitable for industrial processing; however, some insect species can be used, due to the accumulation of a large amount of chitin-containing material that is suitable for industrial manufacturing. These insects can be reared under controlled laboratory conditions such as honeybees, silkworms, and flies (Zhang *et al*., 2000).

In this regard the beetle, *Holotrichia parallela* species was found to possess a chitin content of about 15 %, meaning that this insect considered a good source of chitin (Liu *et al.*, 2012). The weight of the worker honeybee in a colony varies, from 3.5 to 4 kg on average. Every spring, beekeepers get rid of about 20000 tons of naturally dead bees. Thus, this source could yield about 3000 tons of chitin of excellent quality yearly.

A bee family is renewed by 60–80% in spring. So, due to winter dies of the worker bees, the annual volume of bee corpses reaches 6000–10000 ton (Zbigniew Draczynski, 2008). Chitosan nanoparticles prepared by ionic gelation method using TPP were loaded with different animal venoms to investigate their biological efficacy. A nanoparticulate system of chitosan was loaded with *Mesobuthus eupeus* scorpion venom found to have a good alternative to adjuvant systems (Mohammadpour Dounighi *et al.*, 2012 a). Also, nano chitosan prepared from *Lucilia cuprina* maggots were noticed to have a powerful antibacterial potential (Mostafa *et al.*, 2016).

By performing a search on "Scopus" and "Nano.Nature.com", we did not find any reported work on bee venom loaded nano chitosan preparation and / or antimicrobial activity (Figs. 1, a & b).

The present study aimed to extract chitosan from corpses of naturally died honeybees (*Hymenoptera*- Apidae). One of our goals is to prepare bees chitosan nanoparticles (B-CS-NPs). Also, we investigate the loading of nanoparticles with the honeybee, *Apis mellifera* venom (BV-loaded NPs), assess the antimicrobial activity of both (BV), (B-CS-NPs), and (BV-loaded NPs) on Gram-positive, Gram-negative bacteria and fungus models.

Fig (1): Search results of any reported work on bee venom loaded nano chitosan preparation and / or antimicrobial activity on **(A):** Nano.nature.com and **(B):** Scopus

MATERIALS AND METHODS

1. Raw Materials:

Corpses of naturally died honeybees, *Apis mellifera* (Hymenoptera: Apidae) were collected from different apiaries at spring as a natural fall in the beehives were used as a raw material.

2. Extraction of Chitin and Chitosan:

The naturally died bees were dried at 60ºC for a week before being chemically treated. Then they were subjected to successive five stages of treatment (Marei *et al.*, 2016). (Fig. 2)
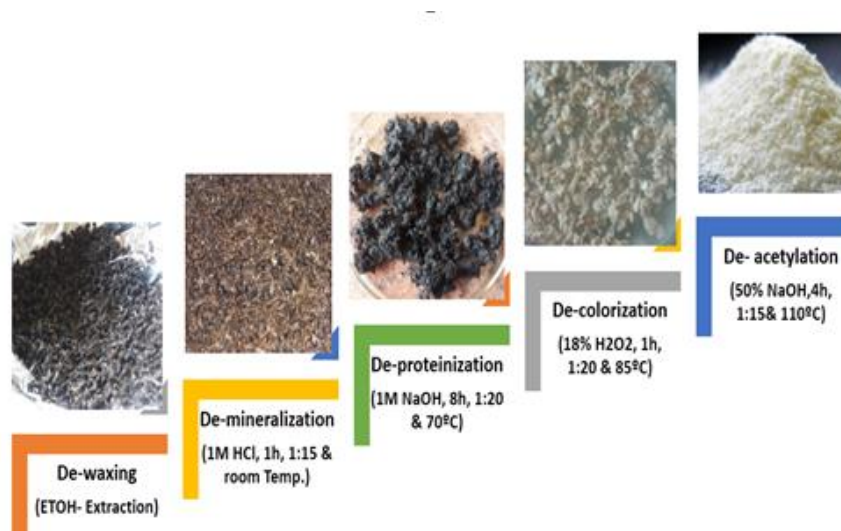
Fig (2): Schematic representation of chitin and chitosan extraction process

3. Preparation of Bee Chitosan Nanoparticles (B-CS-NPs) and Bee Venom Loaded Chitosan Nanoparticles (BV loaded CS-NPs):

Bee Chitosan Nanoparticles (B-CS-NPs) were prepared by ionic gelation of bee Chitosan (B-CS) with trisodium polyphosphate (TPP). For plane (Empty) nanoparticles, TPP (11 ml of 0.33 mg/ml) were dropwisely added during stirring (1000 rpm for 75 minutes) to 0.2 gm of (B-CS) dissolved in 1 % acetic acid. For bee venom loaded nanoparticles (BV Loaded CS-NPs), 20, 50, 100, 200, 400 and 600 µg / ml of bee venom was added to chitosan solution just before adding TPP and at strong acidic pH (Marei, 2014). Both Plane (Empty) and loaded NPs were separated by centrifugation at 14000 rpm for an hour, freeze-dried at -40°C and 0.05 mbar then stored at 4°C ± 2°C. The weight of both loaded and empty NPs was recorded.

4. Characterizations:

4.1. Moisture Content (MC):

The moisture content of the prepared (B-CS) was determined by gravimetric method, in which the water mass was determined by drying the sample in an oven for 24 h at 110°C (**Klute**, **1986**).

4.2. Ash Content (AC):

After incinerating the sample in a muffle furnace for 3 h at 650°C, the ash content was estimated gravimetrically (Rødde *et al.*, 2008).

4.3. X-ray Powder Diffraction (XRD):

To estimate the crystallinity of chitin and chitosan prepared from honeybees, XRD analysis was carried out using a PANalyticalX'Pert machine (Netherland) (Islam *et al*., 2011).

4.4. Fourier Transform Infrared Spectroscopy (FTIR):

Dried bee chitin (B-CT) and chitosan (B-CS) were mixed with KBr, then pressed to form 0.5 mm disc. FTIR spectra in the region from 4000 to 500 cm^{-1} were determined using a Nicolet Avatar 360 spectrophotometer.

4.5. Hydrodynamic Diameter And Zeta Potential:

The hydrodynamic diameter of Plane (empty) and BV loaded NPs was examined using Malvern Zeta sizer (Malvern Instruments, UK) with a wavelength of 532 nm at 25°C with an angle detection of 90°. A definite amount of nanoparticles were prepared in double distilled water and sonicated in an ice bath. 0.1 ml of the NPs suspension was diluted to 1 ml in water and subjected to measurement. The same instrument measured the zeta potential.

Measurements were made at 25°C without sample dilution. All measurements were performed in triplicate (Sagheer *et al*., 2009).

4.6. Microstructure Investigations:

Microstructure investigation of prepared nanoparticles was determined using a transmission electron microscope (TEM) (Philips 400, kV 80; Eindhoven, Netherland). The samples were dispersed in the ultrasonic bath for 20 minutes on copper-coated carbon grids, dried at room temperature, and then examined by TEM (Saeed *et al*., 2013).

4.7. Determination of Venom Loading Capacity (LC) and Encapsulation Efficiency (EE):

Bradford method was used to determine the protein (venom) concentration at 595nm. Samples were centrifuged at 14000 rpm for 1 h at 4°C. Bee venom encapsulation efficiency was calculated as the difference between the total amounts of the venom added in the nanoparticle solution and the amount of non-entrapped venom remaining in the clear supernatant after the centrifugation. The bee venom encapsulation efficiency (EE) and loading capacity (LC) were calculated according to the following equations (Saeed *et al*., 2013):

$$\text{EE \%} = \frac{\text{Total amount of venom} - \text{Free amount of venom}}{\text{Total amount of venom}} \times 100 \qquad (1)$$

$$\text{LC \%} = \frac{\text{Total amount of venom} - \text{Free amount of venom}}{\text{Nanoparticles weight}} \times 100 \qquad (2)$$

4.8. Bee Venom Release from Nanoparticles (*In vitro* release assessment):

In-vitro release profile of bee venom from NPs was carried out by dissolving a definite amount of NPs in release medium (0.01 M PBS, pH 7.4). 1 ml of nanoparticulate suspension was put in separate tubes. The tubes were kept in a shaker at 37°C and 200 rpm. At different time intervals (2, 4, 6, 8, 10, 12, 24, 48 and 72 hours) one tube was removed and the sample was centrifuged at 14,000 rpm and 4°C for 30 minutes. The amount of BV released in the supernatant was measured using the Bradford protein assay (Van der Lubben *et al*., 2013).

5. Determination of Antimicrobial Activity:

Test Organisms:

The antimicrobial activity of BV, B-CS-NPs and BV loaded CS-NPs was evaluated against two strains of G$^+$ (*Bacillus subtilis*, *Staphylococcus aureaus*, ATCC 12600), two strains of G$^-$ (*E. Coli* and *Pseudomonas auriginosa*, ATCC 11775) and 2 fungus models (*Aspergilus flavous* Link and *Candida albicans*, ATCC 7102).

5.1. Disc Diffusion Method:

Antimicrobial activity of the tested samples was determined using a modified Kirby-Bauer disc diffusion method (Bauer *et al*., 1966). 100 µl of the test bacteria/fungi were grown in 10 ml of fresh media until they reached a count of approximately 10^8 CFU /ml for bacteria or 10^5 cells/ml for fungi (Pfaller *et al.,* 1988). 100 µl of microbial suspension was spread onto agar plates corresponding to the broth in which they were maintained. Isolated colonies of each pathogenic organism were selected from primary agar plates and tested for susceptibility by disc diffusion method (National Committee for Clinical Laboratory Standards, 1993). Plates inoculated with filamentous fungi *(Aspergillus flavus)* at 25°C for 48 hours; Gram (+) bacteria (*Staphylococcus aureus, Bacillus subtilis)*; Gram (-) bacteria (*Escherichia coli*, *Pseudomonas aeuroginosa) then*, incubated at 35-37°C for 24-48 hours. Yeast (*Candida albicans)* incubated at 30°C for 24-48 hours and, then the diameters of the inhibition zones were measured in millimeters ((National Committee for Clinical Laboratory Standards, 1993). Standard discs of Antibacterial agent (Ampicillin), Antifungal agent (Amphotericin B) used as positive controls for antimicrobial activity but filter discs impregnated with 10 µl of solvent (distilled water, chloroform, DMSO) were used as a negative control. Standard blank paper disks (8 mm in diameter) were separately soaked in each sample then transferred on to the surface of growth media previously seeded with the

test organisms. The area of no growth around the disc is known as a "Zone of inhibition".

5.2. Determination of Minimum Inhibitory Concentration (MIC):

Micro broth dilution method, using 96 well microtiter plates, was performed to evaluate MIC of BV, B-CS-NPs and BV loaded CS-NPs (Andrews, 2001). An inoculum suspension was prepared in Mueller–Hinton broth. The inoculate were adjusted to each bacterial strain to yield a cell concentration of 108 CFU/ml. A final volume of 200 μl was achieved in each well (180 μl bacterial suspensions and 20 μl of sample). Two control wells were maintained for each test batch. These included test control (well-containing sample and the growth medium without inoculum) and organism control (the well containing the growth medium and the inoculum). The lowest concentration (highest dilution) of the sample that produced no visible bacterial growth (no turbidity) when compared with the control wells were regarded as MIC.

RESULTS AND DISCUSSION

Characterization of Bee Chitosan:

1. Moisture Content:

The performance of the powder used for formulations of pharmaceutical tablets is affected mostly by moisture content. The moisture content of commercial chitosan ranges from 7 to 11% (w/w). The chitosan moisture content is not dependent on the degree of deacetylation and molecular weight. The moisture content of commercial chitosan ranges from 7 to 11 % w/w (Fini, and Orienti, 2003). The moisture content was calculated from the following equation (Kaya *et al.*, 2014):

$$\text{Moisture content (MC) \%} = \left(\frac{W1 - W2}{W1} X100\right) \tag{3}$$

Corpses of naturally died honey bees was found to contain 16.4% moisture.

2. Ash Content:

Degradation of chitosan by heating in the presence of air resulted in the inorganic residue was defined as ash. It is considered as a vital indicator for the demineralization step and effectiveness for the removal of calcium carbonate. Demineralization resulted in products having 31–36% ash. Chitosan of high-quality grade should have less than 1% of ash content (Bough *et al.*, 1971). The ash content (AC) of the chitosan extracted from honey bee corpses was calculated from the equation:

$$\text{Ash content (AC) \%} = \left(\frac{W2}{W1} X100\right) \tag{4}$$

Where W1 and W2 are the weights (in grams) of the initial sample of chitosan and residue, respectively (Khan *et al.*, 2002).

Chitosan extracted from honey bee corpses was showed 7.3% ash content (AC).

3. Degree of De-Acetylation (DDA):

The most important factor that affects different properties of chitin/chitosan is deacetylation degree (DD). DD depends on the way of extraction and conditions of the reaction that should be taken into consideration prior to the use of chitosan as a drug delivery system. The degree of chitin de-acetylation to chitosan was calculated from FTIR spectrum with the following equation (Kasaai, 2008):

$$\text{Deacetylation degree (DDA) \%} = 100 - \left(\frac{A_{1630}}{A_{3430}} X \frac{100}{1.33}\right) \tag{5}$$

Where A_{1630} and A_{3430} are the FTIR absorption bands at 1630 and 3430 cm^{-1}, respectively. Chitosan prepared from bee corpses recorded 78.6% DD.

4. X-ray Diffraction of Chitin and Chitosan:

The XRD profiles of chitin and chitosan are shown in Figures. 3 a,& b .The objective of the XRD studies was to determine the effect of the de-acetylation and grinding treatment

on the crystallographic structure of chitosan. The diffraction patterns of chitin exhibited one intense peak at $2\theta = 19.31$ (110), and another one at $2\theta = 9.33$ (020). Moreover, upon the de-acetylation treatment, the Bragg angle (θ) position is shifted. From the XRD pattern, chitosan exhibited two distinct peaks at $2\theta = 9.75$ (020) and $2\theta = 19.92$ for (110) peak. The crystallite size (*L*) of chitosan from (020) plans becomes smaller after the de-acetylation and grinding processes while that calculated from (110) plan become larger. Taking into account the d-spacing values for the chitin and chitosan, the later presented the smaller d-spacing if compared with chitin (Mogilevskaya *et al.,* 2006). The crystallinity index (*CrI*) of both chitin and chitosan were found to be 91.22% and 79.5%, respectively Table. 1. The difference in *CrI* between chitin and chitosan could be attributed to the grinding process of chitin as was previously described by (Ioelovich, 2014).
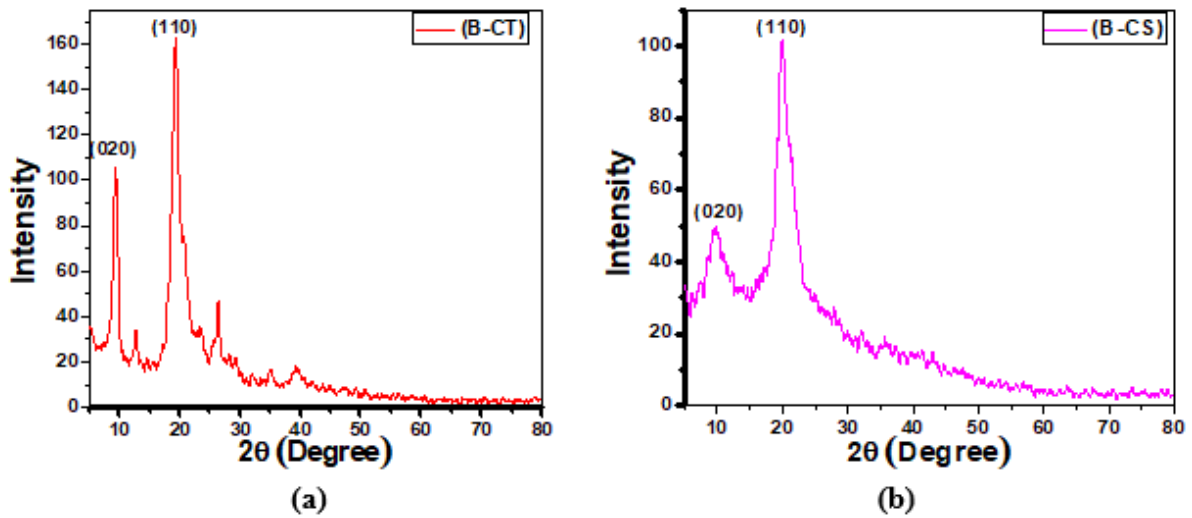
**Fig (3):** XRD pattern of **(a)**: Chitin and **(b):** Chitosan

Table (1): Diffraction angel ($2\theta^\circ$), crystallite sizes (*L*), and d-spacing between the   crystal planes of chitin and chitosan

Sample	$2\theta^\circ$	d-spacing (Å)	(hkl)	L (Å)	CrI
B-CT	9.33	9.48	(020)	231.54	91.22
	19.31	4.60	(110)	194.14	
B-CS	9.75	9.08	(020)	71.45	79.5
	19.92	4.46	(110)	145.13	

5. FTIR Spectroscopy Analysis:

The infrared spectra of bee chitin (B-CT) and chitosan (B-CS) are shown in Figure 4. The FTIR bands assignments which contain the main infrared spectral differences that allowed us to identify the structural changes in these samples are illustrated in Table (2). The strong and wideband in the 3500-3300 area is attributed to hydrogen-bonded O-H stretching vibration and the overlapped N-H stretching from amide I and amide II. The C-N stretching vibration of type I amine appeared at 1317 cm^{-1}, while the band at around 1150 cm^{-1} is assigned for an asymmetric stretch of C-O-C (Gylienë *et al.*, 2003). Asymmetric stretching vibration of CH (-CH2) was observed at band around 2926 cm^{-1} (Zvezdova, 2010). According to the present results, the stretching of hydroxyl groups of C-OH was observed at

bands around 1084 cm^{-1} and 1037 cm^{-1}. The stretching of pyranose skeletal ring has appeared at band 896 cm^{-1} (Zhang *et al.*, 2011). The bending vibration of CH (-CH2) was represented at bands around 1424 cm-1 and 1381cm-1, the bending vibration of CH (-CH2) was represented at bands around 1424 cm^{-1} and 1381cm^{-1} (Liu *et al.*, 2013).
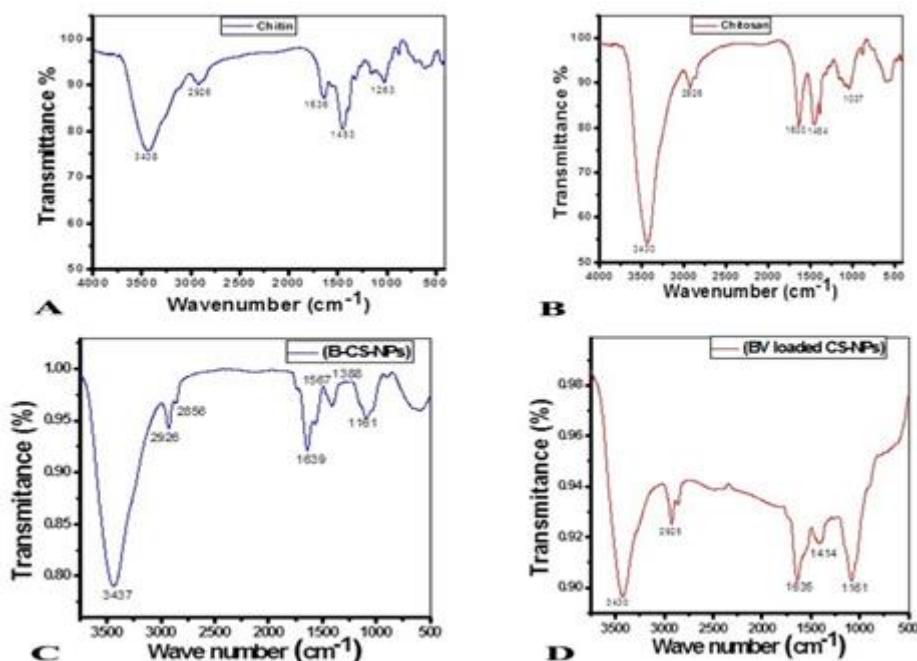
Fig (4): FTIR spectra of **(A):** Bee chitin (B-CT), **(B):** Bee chitosan (B-CS), **(C):** Empty nanoparticles (B-CS-NPs) and **(D):** BV loaded nanoparticles (BV loaded NPs).

Table (2): FTIR band assignments of bee chitin (B-CT) and bee chitosan (B-CS)

Band assignment	Band position (cm^{-1})	
	B-CT	B-CS
ω(C–H) from the polysaccharide's structure	879	880
vC-O	1024	1037
vC-O	1120	1084
v$_{as}$C-O-C	1157	1152
v(C-O-H)	1263	-
v$_s$(CH$_3$) of amide III	1319	1318
δ (C-H), v(-NH) of amide III	1390	1388
δ(C-H)	1453	1454
v(-C=O) of amide II	1552	-
v(-C=O) of amide I & δ H$_2$O	1636	1630
v$_s$(C-H)	2856	2856
v$_{as}$(C-H)	2926	2926
v(O-H), v(N-H) overlapped	3438	3430

Characterization of Nanoparticles:
   1. Loading Capacity (LC %) and Encapsulation Efficiency (EE %):
          Figure (5) represented Influence of BV initial concentration on encapsulation
efficiency. In the present study, both B-CS and TPP concentrations remained constant (200
mg / ml and 1.1 mg/ml respectively). Different concentrations of bee venom (20, 50, 100,
200, 400, 600 and 800 µg / ml) were used. The results revealed that by increasing of the
venom concentration from 20 to 600 µg/ ml, both % encapsulation efficiency and % loading
capacity increased. Encapsulation efficiency recorded values ranged from 71% to 91.3%,
while loading capacity ranged from 10.2 % to 86.5 %. (Table3). This high EE can be
explained because the venom is dissolved in TTP solution and at the moment of cross-linked
nanoparticle formation, these protein molecules are completely trapped inside the polymeric
matrix of chitosan nanoparticles (Gan and Wang, 2007). Moreover, the electrostatic
interactions between positively charged groups of chitosan and negatively charged proteins
are frequent during the formation of nanoparticles and other part adsorbed on the surface of
nanoparticles (Gan *et al*., 2005).Optimum loading capacity and encapsulating efficiency of
venom were obtained with venom concentration of 600µg/ml. More than 90% of EE was
obtained at different *Tityus serrulatus* scorpion venom: chitosan ratios (5 and 10%) (Orkideh
et al., 2013). Also, venom EE and LC were significantly affected by the initial *Echis
carinataus* snake venom concentration. The loading efficiency increased from 71% to 89%
and LC also increased from 12% to 82% as the concentration of venom increased during
conjugation with chitosan nanoparticles [l]**.** Additionally, EE of Russell's viper snake venom
conjugated with chitosan nanoparticles was 89% at concentrations of 1000 µg/mL of venom
and 2mg/ml of chitosan (Venkatesan *et al.,* 2013).
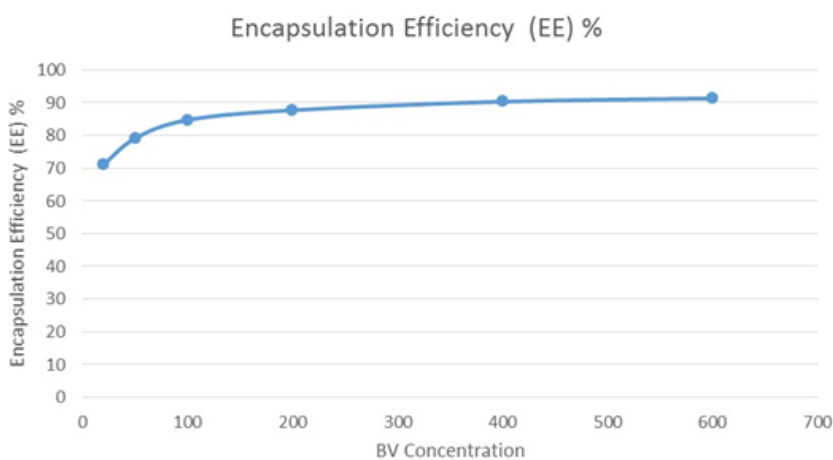
Fig (5): Influence of BV concentration on encapsulation efficiency of chitosan nanoparticles.

Table: (3): Effect of bee venom concentration on encapsulation efficiency and loading
        capacity of bee venom on chitosan nanoparticles

BV Concentration (µg / ml)	Loading capacity (LC) %	Encapsulation Efficiency (EE) %
20	10.2	71
50	28.4	79.1
100	42.7	84.7
200	57.6	87.7
400	72.1	90.3
600	86.5	91.3
800	108.1	91

2. Hydrodynamic Diameter:

The hydrodynamic diameters of empty (B-CS-NPs) Figure. 6, a and 600 μg / ml BV loaded-CS-NPs Figure 6, b were 74.2 nm to 110.5 nm respectively, possibly because of the large size and molecular weight of protein, venom adsorption on nanoparticles surface during the incubation period and negligible increase of viscosity by venom during loading of nanoparticles. Also, the hydrodynamic diameter of *Echis carinataus* snake venom loaded nanoparticles (116 nm) was larger than chitosan nanoparticles (89 nm) when evaluated by DLS (Dounighi *et al.,* 2015). In contrast, the size of *Tityus serrulatus* scorpion venom loaded nanoparticles was smaller than chitosan nanoparticles, where the average size was 180 and 149.6 nm for chitosan nanoparticles and venom loaded nanoparticles, respectively (Rocha Soares *et al.,* 2013).
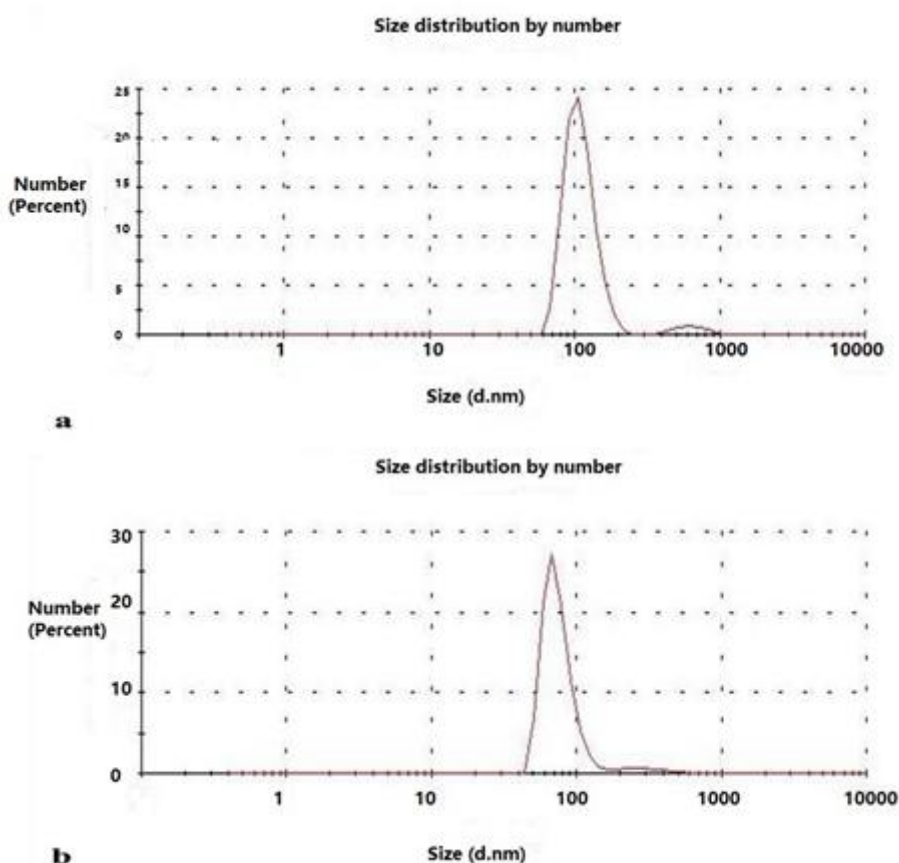

Fig (6): Hydrodynamic diameters of **(a):** empty chitosan nanoparticles and **(b):** BV loaded chitosan nanoparticles (Chitosan 2mg/ml, TPP 1.1 mg/ml and BV 600 μg / ml).

3. Zeta Potential :

Figures. 7; a,& b illustrated respective zeta potentials of empty and bee venom-loaded nanoparticles that were prepared at the optimum concentrations of bee venom (2mg/ml chitosan with 600 μg/ml of venom) with an encapsulation efficiency of 91.3 % and loading capacity of 86.5 %. The values of zeta potentials were 51.1 mV and 49.0 mV for empty and bee venom loaded nanoparticles respectively demonstrating that the venom loading leads to a minor reduction of the particle's zeta potential. Zeta potential is quite important for colloids and nanoparticles in suspension. Its value is closely related to suspension stability and particle surface morphology (Gan and Wang, 2007). Zeta potential of the chitosan loaded nanoparticles can greatly influence their stability in media through electrostatic repulsion between the particles. The present results indicated that zeta potential analysis, in which the

increment or addition of protein leads to a decrease in the positive charge on the particle surface 51.1 mV of empty nanoparticles only to 49.0 mV by loading the bee venom. This reduction can be due to the interaction of venom with polymer and molecules of venom adsorbed on the surface of the particles (Zhang *et al.,* 2011). The carboxyl groups on the surface of the large protein molecules may form hydrogen bonds with amine groups at certain sites at the chitosan chain but, still maintaining a compact 3-D structure without spreading at the solution pH condition (pH 3.5) so as to keep an inner hydrophobic core. Therefore, protein molecule attachment did not sufficiently suppress the positive surface charge of chitosan molecules, when the zeta potential profile of chitosan nanoparticles is compared with the zeta potential of chitosan nanoparticles containing bee venom. It still seems that a high proportion of free amine groups on the chitosan chain remained unoccupied. Also, the zeta potential was decreased from 42.37 mV to 24.34mV by loading *Tityus serrulatus* scorpion venom on chitosan (Rocha Soares *et al.,* 2012). In this regard, the zeta potential of *Mesobuthus eupeus* scorpion venom-loaded chitosan nanoparticles and empty ones recorded 50.3 mV and 44.1 mV, respectively (Mohammadpour Dounighi *et al.*, 2012 b).
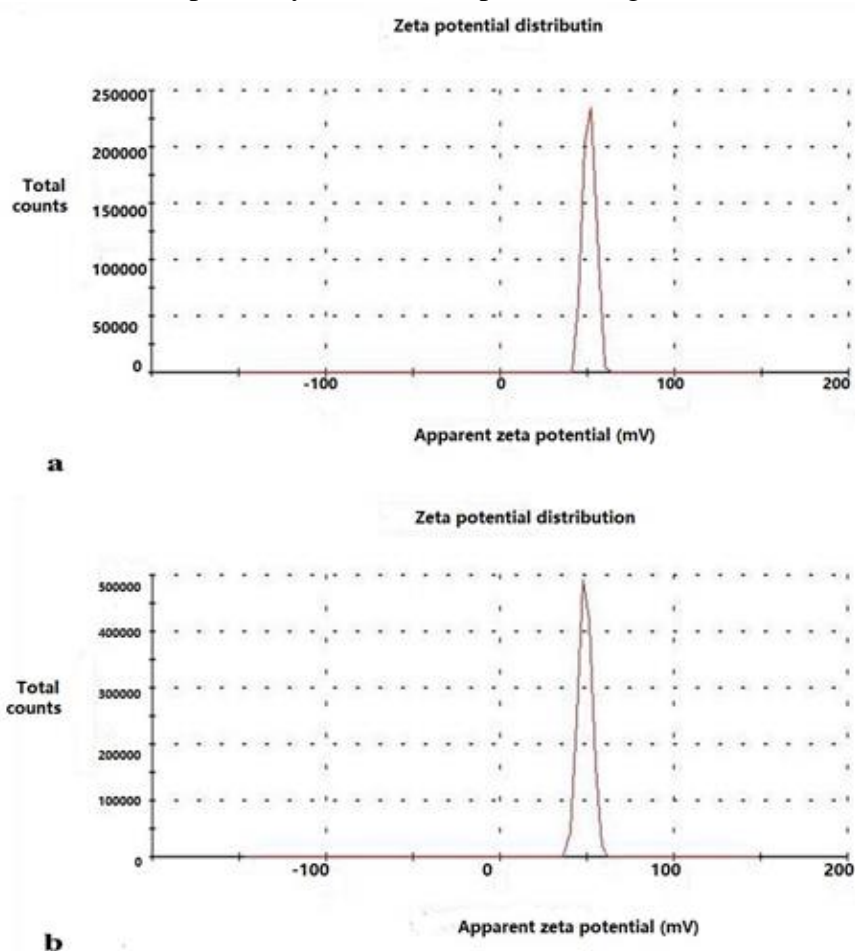
Fig (7): Zeta potential analysis of **(a):** empty nanoparticles   and **(b):** BV loaded NPs. (2 mg/ml chitosan, 1.1 mg/ml TPP and 600 µg / ml BV)

4. Microstructure investigation using transmission electron microscope (TEM)

Figures. 8 a, & b represented transmission electron microscope (TEM) micrographs of empty nanoparticles and bee venom-loaded chitosan nanoparticles that were prepared at optimum concentrations of bee venom (2mg/ml chitosan and 1.1 mg/ml TPP with 600µg/ml of venom). TEM images showed that nanoparticles have a smooth surface and spherical shape. The size range of prepared nanoparticles was about 80-155 nm**.**
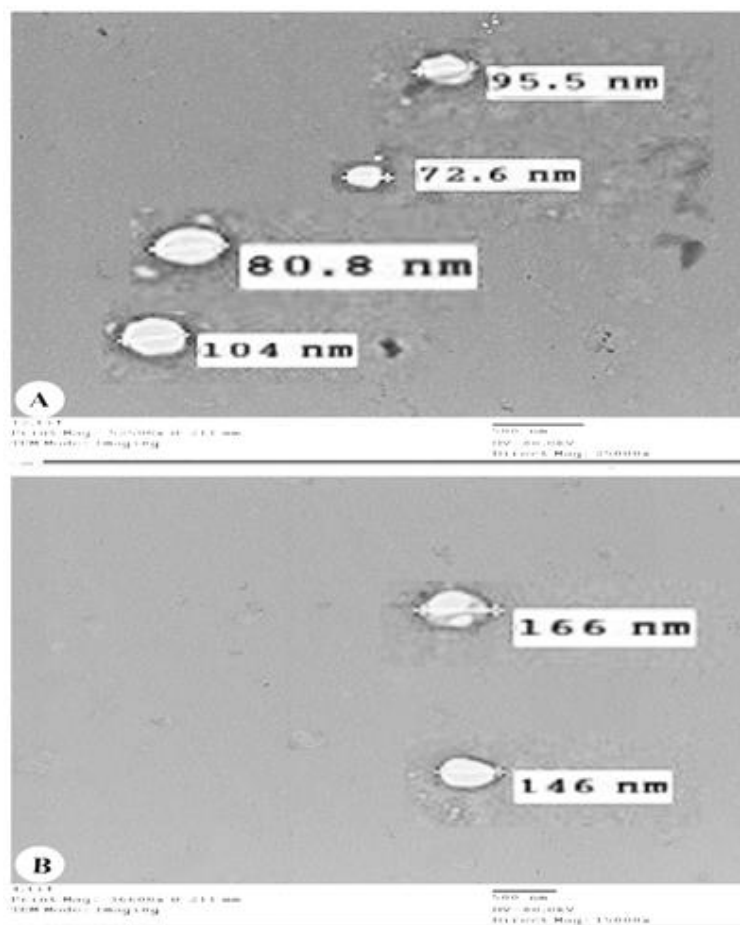
Fig (8): TEM image of empty nanoparticles (A) and BV loaded nanoparticles

5. FTIR

FTIR spectroscopy (Fig. 4) revealed that all CS samples (empty NPs and BV loaded NPs) have similar chemical composition. This is an indication that BV didn't largely affect CS-NPs bands (Taher *et al.*, 2017). In empty nanoparticles (B- CS-NP), the band of 3430 cm^{-1} has a shift to 3437 cm^{-1} and become wider. The bands for N-H bending vibration of amide I and the amide II appeared at 1639cm^{-1}, and 1567cm^{-1}, respectively. The intense band at 1388cm^{-1} was caused by -NH stretching of amide III in the fingerprint region of the spectra; symmetric stretching of C-O-C was observed around 1088cm^{-1}. Absorption band for carbonyl (C=O) stretching of the amide II was observed near 1658 cm^{-1}. The band in the region of 880cm^{-1} was caused by the saccharide structure of CS. A P=O band from CS-NPs cross-linked with TPP appeared at 1161 cm^{-1}. The appearance of such band is an indication of possible ammonium ion, from CS-NPs, linkage with tripolyphosphoric groups, from TPP, Thus the inter- and intra-molecular actions are enhanced in CS-NPs (Mohammadpour Dounighi *et al.*, 2012 b). The FTIR spectra of bee venom loaded CS-NPs demonstrated that stretching vibrations of -OH and -NH$_2$ at 3430 cm^{-1} were broader. The intense band at 1414 cm^{-1} belonged to C-N stretching. For venom loaded CS-NPs, the 1639 cm^{-1} band of amide I shifted to 1635 cm^{-1} perhaps because of the cross-linking between BV venom and CS-NPs. The P=O band position from B-CS-NPs remains virtually unchanged at 1161cm^{-1} (Mirzaei *et al.,* 2017). (Table. 4).

Table (4): FTIR band assignments of bee chitosan nanoparticles (B-CS-NPs) and bee venom loaded chitosan nanoparticles (BV loaded CS-NPs)

Band assignment	Band position (cm^{-1})	
	B-CS-NPs	BV loaded CS-NPs
ω(C–H) from the polysaccharide's structure	898	902
νC-O	1088	1082
νP=O	1161	1161
ν(C-O-H)	1259	1258
ν_s(CH$_3$) of amide III	-	1323
ν(C-N)	1411	1407
ν(-C=O) of amide II	1567	-
ν(-C=O) of amide I & δ H$_2$O	1639	1635
ν_s(C-H)	2862	2860
ν_{as}(C-H)	2927	2925
ν(O-H), ν(N-H) overlapped	3437	3430

6. *In vitro* Release Study:

In vitro release profile of venom loaded nanoparticles (Table 5) showed that in the first 12 hrs of incubation, about 67.1 % of the venom released followed by a slow release of 15.9 % during the subsequent 12 hrs. The release process involved two different mechanisms, the diffusion of protein molecules and the degradation of the polymer matrix. Initial burst release of the venom was due to the venom molecules that dispersing close to the nanoparticles surface, which easily diffuse in the initial incubation time, followed by sustained release phase, which was due to the slow degradation of nanoparticles leading to the release of entrapped venom with a constant rate (Zhou and Li., 2001). About 60.9% of cisplatin loaded chitosan nanoparticles [42] was released at the end of a 12 hour period (Serpil *et al.,* 2015). Also**,** about 90% of the loaded venom released within 72 hrs of incubation in phosphate buffered saline (PBS). The release profile of *Mesobuthus eupeus* venom loaded nanoparticles exhibited an initial burst release of about 60% in the first 10 hrs followed by a slow release of 30% at the subsequent 62 hrs (Mohammadpour Dounighi *et al*., 2012 b). In this regard, in the first 31 hrs of incubation, about 31% of the *Orthochirus iranus* scorpion venom was released, followed by a very slow venom release (Mohammadpour Dounighi *et al*., 2015).

Table (5): Relationship between bee venom release % from nanoparticles and time intervals (Hrs)

Time intervals (Hrs)	Venom release %
2	10.4
4	15.3
6	17.1
8	51.3
10	60.9
12	67.1
24	83
48	81.2
72	80.1

7. *In vitro* Antimicrobial Activity:

All tested samples showed good antimicrobial activity against tested microorganisms except *Aspergillus flavus* fungus, which didn't affect when compared with the high concentration of loaded samples (Fig. 9). Empty nanoparticles with the highest concentration (2 mg / ml CS, 1.1 mg / ml TPP) exhibited different inhibition zones (10 - 14 mm) against gram-positive, gram-negative and fungal test organisms. On the other hand, BV loaded Cs-NPs with the highest concentration (2 mg / ml CS, 1.1 mg/ml TPP and 600 µg / ml BV) exhibited different inhibition zones (11 - 14 mm) against gram positive, gram negative and fungal test organisms also, (Table 6) .

Fig (9): Antimicrobial activity of empty NPs and BV loaded NPs against gram positive bacteria, gram negative bacteria and fungal models

Table (6): Mean diameters of inhibition zones of BV, empty nanoparticles and bee venom loaded nanoparticles against Gram positive bacteria, Gram negative bacteria and fungi test microorganisms

Sample	Inhibition zone diameter (mm / sample)					
	Bacteria				Fungi	
	(G$^+$)		(G$^-$)			
	Bacillus subtilis	*Staphylococcus aureus*	*Escherichia coli*	*Pseudomonas aeruginosa*	*Aspergillus flavus*	*Candida albicans*
BV	13	15	16	13	9	13
B-Cs-NP	13	14	14	14	0.0	10
BV-Loaded Cs-NP	12	14	13	13	0.0	11

MIC results (Table 7) revealed that BV loaded NPs inhibited the growth of tested micro-organisms more efficiently than empty nanoparticles or BV itself, except in case of *Aspergillus flavus* fungus who was resistant to empty and loaded nanoparticles than BV itself. These findings may be due to increasing the penetration of BV sustainably released from nanoparticles into the bacterial cell then inhibited the microbial growth. Increasing the antimicrobial activity of BV loaded on CS nanoparticles, could not be due to the antimicrobial effect of CS nanoparticles alone, because the CS nanoparticles have inhibitory effect at high concentrations. MIC of ciprofloxacin loaded chitosan nanoparticles was 50% lower than that of ciprofloxacin hydrochloride alone in both of tested microorganisms (Zahra *et al.*, 2017). Several mechanisms for the antimicrobial action of chitosan have been postulated. There are as follows: (1) Chitosan could be chelated with trace elements or essential nutrients so as to inhibit the growth of bacteria (Roller *and* Covill, 1999); (2) Chitosan could interact with anionic groups on the cell surface and form polyelectrolyte complexes with bacterial surface compounds [46] thereby forming an impermeable layer around the cell, which prevents the transport of essential solutes into the cell (Bong et al., 2001). Antibacterial effect of silver nanoparticles associated with chitosan is more effective against Gram-negative than Gram-positive bacteria, probably due to the differences in cell walls (Priscila *et al.,* 2016). The Gram-positive bacteria have a cell envelope of lipoteichoic acid along with a thick peptidoglycan layer and the cell membrane. This thick peptidoglycan layer (30–100 nm thick) protects the cells against the penetration of silver ions and injurious reagents into the cytoplasm (Mishra *et al.*, 2015). In contrast, the cell envelopes of Gram-negative bacteria consist of a thin peptidoglycan layer and a cell membrane; hence, they are more susceptible to penetration of AgNPs (Silhavy *et al.,* 2015). Chitosan with silver nanoparticles interacts with the bacterial cell wall forming pits, which promote the escape of molecules of essential membrane proteins and lipopolysaccharide in Gram-negative bacteria, which leads to cell death (Raghavendra *et al.*, 2016). Doping of chitosan with nanoparticles enhanced the antibacterial properties and improved the bactericidal efficiency. All tested bacteria were susceptible to a much lower concentration of chitosan, irrespective of its molecular weights, when combined with the silver nanoparticles (Raghavendra *et al.*, 2016). Also, silver nanoparticles immobilized in a Chitosan nanocarrier interacted strongly with the bacterial surface due to their high surface area and reactivity, thereby causing disruption of membrane integrity. The Ag NPs inside the nanocarrier also disrupted the membrane integrity leading to increased permeability of the membrane leading to leakage of proteins and other intracellular constituents leading to killing of bacteria.

Table (7): Minimum inhibitory concentrations (MIC) of BV, empty nanoparticles and BV loaded nanoparticles against Gram positive bacteria, Gram negative bacteria and fungi test microorganisms

Microorganism			MIC (µg /ml)		
			BV	CS-NP	BV-Loaded-NP
Bacteria	G+	*Bacillus subtilis*	124	188	49.2
		Staphylococcus aureus	240	148	31.2
	G-	*Escherichia coli*	88	132	33.6
		Pseudomonas aeruginosa	164	124	32.4
Fungi		*Aspergillus flavus*	640	Not detected	Not detected
		Candida albicans	410	692	180

Conclusion:

According to the present results, chitosan was extracted successfully from the corpses of naturally died honeybees. Nanoparticle was prepared from bee chitosan and loaded with bee venom exhibited antimicrobial activities against the growth of tested Gram-positive, Gram-negative bacteria and fungal models. MIC of BV loaded NPs was lower when compared to BV alone or empty nanoparticles in all tested microorganisms, except in case of *Aspergillus flavus* fungus which had no response towards empty and BV loaded nanoparticles. The effectiveness of BV was enhanced using CS nanoparticles and is promising for clinical studies as an antimicrobial agent.

Conflict of Interest:

On behalf of all authors, I report the following information with our submission:

1. No third-party financial support for the work in the submitted manuscript.

2. No financial relationships with any entities that could be viewed as relevant to the general area of the submitted manuscript.

3. No sources of revenue with relevance to the submitted work who made payments in the 36 months prior to submission.

4. No interactions with the sponsor of outside of the submitted work should also be reported.

5. No relevant patents or copyrights (planned, pending, or issued).

6. No other relationships or affiliations that may be perceived by readers to have influenced, or give the appearance of potentially influencing, what you wrote in the submitted work.

REFERENCES

Andrews, J.M (2001): Determination of minimum inhibitory concentrations. *J Antimicrob Chemother.*1:5-16.

Bauer AW, Kirby WM, Sherris C, Turck M, (1966): Antibiotic susceptibility testing by a standardized single disk method, American Journal of Clinical Pathology, 45, 493-496.

Bong, K. C., Kwang-Yoon, K., Yun-Jung, Y., Suk-Jung, O., Jong-Hoon, C., Chong-Youl, Kim. (2001): In vitro antimicrobial activity of a chitooligosaccharides mixture against *Actinobacillus actinomycetemcomitans* and *Streptococcus mutans*. International Journal of antimicrobial agent. 18, (6): 553-557.

Bough, W., Salter, W., Wu, A., and Perkins, B. (1978): Influence of manufacturing variables on the characteristics and effectiveness of chitosan products. I. Chemical composition, viscosity, and molecular weight distribution of chitosan products, Biotechnology and Bioengineering 20, 1931 – 1943.

Dounighi, M.N.; Mehrabi, M.; Avadi, M.R.; Zolfagharian, H. and Rezayat, M. (2015): Preparation, characterization and stability investigation of chitosan nanoparticles loaded with the *Echis carinatus* snake venom as a novel delivery system. Archives of Razi Institute, 70 (4): 269-277.

Fini, A., and Orienti, I. (2003): The role of chitosan in drug delivery, Am. J. drug deliv. 1, 43 – 59.

Gan, Q. and Wang, T. (2007): Chitosan nanoparticles as protein delivery carrier-systematic examination of fabrication conditions for efficient loading and release. Colloids and Surfaces B. Biointerfaces, 59(1): 24-34.

Gan, Q. and Wang, T. (2007): Chitosan nanoparticles as protein delivery carrier-systematic examination of fabrication conditions for efficient loading and release. Colloids and Surfaces B. Biointerfaces, 59(1): 24-34.

Gan, Q.; Wang, T.; Cochrane, C. and McCarron, P. (2005): Modulation of surface charge, particle size and morphological properties of chitosan–TPP nanoparticles intended for gene delivery. Colloids and Surfaces *B*. Biointerfaces, 44(2-3):65-73.

Gylienë, O., Razmutë, I., Tarozaitë, R. and Nivinskienë, O. (2003): Chemical composition

and sorption properties of chitosan produced from fly larva shells. Chemija (Vilnius), 14(3), 121-127.

Ioelovich, M. (2014): Crystallinity and hydrophility of chitin and chitosan. *J. Chem* 3 (3): 7-14.

Islam, M.M., Masum, S.M., Rahman, M.M., Molla, A.I.M., Shaikh, A.A., Roy, S.K., (2011): Preparation of Chitosan from Shrimp Shell and Investigation of Its Properties. Int. J. Basic Appl. Sci. 11: 77–80.

Kasaai, M. R. (2008): A review of several reported procedures to determine the degree of N-acetylation for chitin and chitosan using infrared spectroscopy." Carbohydrate Polymers 71 (4): 497-508.

Kaya, M., Baublys, V., Can, E., Sˇatkauskiene, I., Bitim, B., Tubelyte, V., Baran, T. (2014): Differentiations of Chitin Content and Surface Morphologies of Chitins Extracted from Male and Female Grasshopper Species. *Zoomorph, 133: 285–293.*

Khan, T. A., Peh, K.K., and Chng, H.S. (2002): Reporting degree of deacetylation values of chitosan: the influence of analytical methods, J. Pharm Sci. 5, 205-212.

Klute, A. (1986): Methods of Soil Analysis (Part 1); Physical and Mineralogical Methods, American Society of Agronomy, Inc.,

Liu, M.; Zhou, Y.; Zhang, Y.; Yu, C. and Cao, S. (2013): Preparation and structural analysis of chitosan films with and without sorbitol. Food Hydrocolloids, 33(2), 186-191.

Liu, S, J. Sun, L. Yu, C. Zhang, J. Bi, F. Zhu, M. Qu, C. Jiang, and Q. Yang (2012): Extraction and characterization of chitin from the beetle Holotrichia parallela motschulsky. Molecules 17: 4604-4611.

Marei, N. H. (2014): Synthesis and characterization of chitosan nanoparticles from locust *shistocerca gregaria* and other sources and its efficiency as drug delivery system for ciprofloxacin. A thesis submitted in partial fullfilment of Master of Science in biotechnology, Chemistry Department, Faculty of Science, Cairo University. Egypt.

Marei, N. H., E. A. El-Samie, T. Salah, G. R. Saad and A. H. Elwahy (2016): "Isolation and characterization of chitosan from different local insects in Egypt.″ Int J Biol Macromol 82: 871-877.

Mirzaei, F., M. R. Avadi and M. Rezayat (2017): A New Approach to Antivenom Preparation Using Chitosan Nanoparticles Containing Echis Carinatus Venom as A Novel Antigen Delivery System. *Iranian Journal of Pharmaceutical Research 16 (3): 858-867.*

Mishra, S.K., Ferreira, J.M., Kannan, S. (2015): Mechanically stable antimicrobial chitosan-PVA-silver nanocomposite coatings deposited on titanium implants. <u>Carbohydr Polym.</u> 5 (121): 37-48.

Mogilevskaya, E. L., T. A. Akopova, A. N. Zelenetskii and A. N. Ozerin (2006): The crystal structure of chitin and chitosan. Polymer Science Series A 48(2): 116-123.

Mohammadpour Dounighi Naser, Yazdizadeh Rezvan and Zolfagharian Hossein., (2015): A New Antigen Delivery Vehicle Candidate: *Orthochirus iranus* Scorpion Venom Entrapped in Chitosan Nanoparticles. *Br.* J. Pharm. Res., 7 :(4): 264-275.

Mohammadpour Dounighi, N.; Damavandi, M.; Zolfagharian, H. and Moradi, S., (2012 a): Preparing and Characterizing Chitosan Nanoparticles Containing *Hemiscorpius lepturus* Scorpion Venom as an Antigen Delivery System. Arch. Razi Instit., 67(2): 145-153.

Mohammadpour Dounighi, N.; Eskandari, R.; Avadi, M. R.; Zolfagharian, H.; Mir Mohammad Sadeghi, A. and Rezayat, M. (2012 b): Preparation and *in vitro* characterization of chitosan nanoparticles containing *Mesobuthus eupeus* scorpion venom as an antigen delivery system. J. Venomous Anim. Toxins including Trop. Dis. 18 (1): 44-52.

Mostafa I. Hassan, Fatma A. Taher, Aly F. Mohamed & Mohammad R. Kamel. (2016): Chitosan Nanoparticles Prepared from *Lucilia Cuprina* Maggots as antibacterial agent. J. Egypt. Soc. Parasitol. (JESP), 46(3), 519 – 526.

Muzzarelli, R., Tarsi, R., Filippini, O., Giovanetti, E., Biagini, G., and Varaldo, P.G. (1990): Antimicrobial properties of N-carboxybutyl chitosan. *Antimicrob Agents Chemother*. 34(10): 2019–2023.

National Committee for Clinical Laboratory Standards. (1993): Methods for dilution antimicrobial susceptibility tests for bacteria that grow aerobically. Approved standard M7-A3. National Committee for Clinical Laboratory Standards, Villanova, Pa.

National Committee for Clinical Laboratory Standards. (1993): Performance VOL. 41, 1997 antimicrobial susceptibility of Flavobacteria.

Orkideh Ghorban Dadras, Assal Mir Mohammad Sadeghi, Nastaran Farhangi, Nazanin Forouhar ,Naser Mohammadpour, Mohammad Reza Avadi., (2013): Preparation, Characterization and in vitro Studies of Chitosan Nanoparticles Containing Androctonus Crassicauda scorpion venom. J. Appl. Chem. Res., 7(3): 35-46.

Pfaller, M. A., L. Burmeister, M. A. Bartlett, and M. G. Rinaldi. (1988): Multicenter evaluation of four methods of yeast inoculum preparation. J. Clin. Microbiol. 26:1437–1441.

Priscila, L.L., Allan, J.R., Isabela, A.P., Teresinha, G.¸ Jaciana, S., Aguiar, Andr´e. (2016): Antimicrobial and cytotoxicity evaluation of Colloidal Chitosan − Silver nanoparticles − Fluoride nanocomposites. International Journal of Biological Macromolecules. 93 A, 896-903.

Raghavendra, G.M., Jung, J., Kim, D., Seo, J. (2016): Step-reduced synthesis of starch-silver nanoparticles. *Int. J. Biol. Macromol.* 84; 281-288.

Rocha Soares, K.S.; Cardozo Fonseca, J.L.; Oliveira Bitencourt, M.A.; Santos, K. S.C.R.; Silva-Júnior, A.A. and Fernandes-Pedrosa, M.F. (2012): Serum production against *Tityus serrulatus* scorpion venom using cross-linked chitosan nanoparticles as immunoadjuvant. Toxicon, 60 (8): 1349–1354.

Rødde, R.H., Einbu, A., Varum, K.M. (2008): A seasonal study of the chemical composition and chitin quality of shrimp shells obtained from northern shrimp (*Pandalus porealis*). Carbohydr Polym. 71 388–393.

Roller, S., *Covill*, N. (1999): The antifungal properties of chitosan in laboratory media and apple juice. Int. J. Food Microbiol. *47:67–77.*

Saeed Moradhaseli, Abbas Zare Mirakabadi, Ali Sarzaeem, Nasser Mohammadpour dounighi, Saman Soheily, and Mehrasa Rahimi Borumand. (2013): Preparation and Characterization of Sodium Alginate Nanoparticles Containing ICD-85 (Venom Derived Peptides). International Journal of Innovation and Applied Studies. 4: 534-542.

Sagheer, F. A. A., M. A. Al-Sughayer, S. Muslim and M. Z. Elsabee (2009): Extraction and characterization of chitin and chitosan from marine sources in Arabian Gulf. Carbohydrate Polymers 77 (2): 410-419.

Serpil, O., Nisa, Tandogan., Mustafa, Turk., Siyami, Karahan., and Zekiye, Suludere. (2015): The Apoptotic and Necrotic Effects of Cisplatin Loaded Chitosan Nanoparticles on Hela Cell Lines. Academic Journal of Cancer Research, 8 (4): 58-68.

Silhavy, T.J., Kahne, D., Walker, S. (2010): The bacterial cell envelope. Cold Spring Harb Perspect Biol. 2 (2010) http://dx.doi: 10.1101/cshperspect.a000414.

Taher, F. A., W. A. Moselhy, A. F. Mohamed, S. E. E. Didamony, K. M. Metwalley and Z. A. B (2017): Preparation and Characterization of Shrimp Derived Chitosan and Evaluation of Its Efficiency as Bee Venom Delivery for Cancer Treatment. *International Journal of Advanced Research* 5 (5): 370-388.

Van der Lubben I.M.V, Kersten G., Fretz M.M., Beuvery C., Verhoef J.C. and Junginger HE.

(2003): Chitosan microparticles for mucosal vaccination against diphtheria: oral and nasal efficacy studies in mice. Vaccine 21: 1400-1408.

Venkatesan, C.; Vimal, S. and Sahul Hameed, A. S. (2013): Synthesis and Characterization of Chitosan Tripolyphosphate Nanoparticles and its Encapsulation Efficiency Containing Russell's Viper Snake Venom. J Biochem. Mol. Toxicol., 27(8): pp 406-411.

Yang, S.G.; Chang, J.E.; Shin, B.; Park, S.; Na, K. and Shim, C.K. (2010): 99 mTc - hematoporphyrin linked albumin nanoparticles for lung cancer targeted photodynamic therapy and imaging. Journal of Materials Chemistry, 20 (41): 9042–9046.

Zahra, S., Soliman M. S., Hashem, M., Elham, Khezri. (2017): Nanoparticles of Chitosan Loaded Ciprofloxacin: Fabrication and Antimicrobial Activity. *Adv Pharm Bull, 7(3), 427-432.*

Zbigniew Draczynski (2008): Honeybee Corpses as an Available Source of Chitin. l of Appl Pol Sci,. 109, 1974–1981.

Zhang, A; Qin, Q; Zhang, H; Wang, H.; Li, X.; Miao, L. and Wu, Y. (2011): Preparation and characterization of food-grade chitosan from housefly larvae. Czech Journal of Food Science, 29 (6), 616-623.

Zhang, M., Haga, A., Sekigushi, H., Hirano, S (2000): Structure of insect chitin isolated from beetle larva cuticle and silkworm (Bombyx mori) pupa exuvia. *Int. J. Biol. Macromol, 27: 99.*

Zhou, X.M. and Li, X.H. (2001): Investigation on a novel core-coated microspheres protein delivery system. Journal of Controlled Release, 75 (1-2): 27-36.

Zvezdova, D. (2010): Synthesis and characterization of chitosan from marine sources in Black Sea. *Annual Proceedings*," Angel Kanchev" University of Ruse, 49(9.1), 65-69.

ARABIC SUMMARY

"التقييم المعملي للنشاط المضاد للميكروبات لسم نحل العسل (أيبس ميلليفيرا) المحمل علي جزيئات الكيتوزان النانوية"

مصطفي ابراهيم حسن[1]، سماء إمام الدق[2]، علي فهمي محمد[3] و عبدالوهاب خليل عبدالوهاب[4]

1- قسم علم الحيوان وعلم الحشرات ، كلية العلوم ، جامعة الأزهر ، مدينة نصر ، القاهرة ، مصر
2- قسم علوم المواد وتكنولوجيا النانو ، كلية الدراسات العليا للعلوم المتقدمة ، جامعة بني سويف ، بني سويف 62511 ، مصر
3- قطاع البحوث التطبيقية ، هيئة المصل و اللقاح (Vacsera) ، الجيزة ، مصر
4- قسم علم الحيوان ، كلية العلوم ، جامعة بني سويف ، بني سويف ، مصر

كان الهدف من هذه الدراسة هو استخراج الكيتوزان من جثث نحل العسل التالفة بشكل طبيعي ، وإعداد جسيمات كيتوزان النحل النانوية (B- CS- NPs) و تحميل سم نحل العسل عليها وتقييم إمكاناتها المضادة للميكروبات. تم استخراج الكيتين من جليد جثث نحل العسل الميتة بشكل طبيعي في 4 خطوات ؛ إزالة الصمغ ، إزالة المعادن ، إزالة البروتين و إزالة اللون. تم الحصول على الكيتوزان من خلال نزع مجموعة أسيتيل من الكيتين و توصيفه باستخدام الأشعة تحت الحمراء (فورييه (FTIR))و حيود الأشعة السينية. أعدت جسيمات كيتوزان النحل النانوية (B-CS-NPs) بواسطة طريقة دبق الجيل الأيوني باستخدام ثلاثي فوسفات الصوديوم (TPP) في وسط حامضي. تم توصيف كل من الجسيمات الفارغة و المحملة بسم النحل. كان الحجم الهيدروديناميكي و قدرة الزيتا نانومتر 74.2 و 51.1 مللي فولت علي التولي, بينما في حالة الجسيمات المحملة بسم النحل كانت 110.5 نانوميتر و 49 مللي فولت علي التوالي. كانت كانت سعة التحميل وكفاءة التغليف 86.5. ٪ و 91.3 ٪ ، على التوالي و ذلك عند استخدام سم النحل بتركيز 600 ميكروغرام / مل. تمت دراسة النشاط المضاد للميكروبات لكل من الجسيمات النانوية الفارغة والمحملة بسم النحل ضد سلالات مختلفة من البكتيريا المسببة للأمراض البشرية والفطريات و وجد ان : بالمقارنة مع الجسيمات النانوية الفارغة ، أظهرت الجسيمات المحملة بسم النحل نشاطًا قويًا مضادًا للميكروبات محل الدراسة باستثناء فطر اسبيرجلس فلافوس ، الذي ابدي مقاومة.